*Optica Applicata, Vol. LI, No. 2, 2021*
DOI: 10.37190/oa210208

# *Q*-switched partially coherent lasers with controllable spatial coherence

YUSHUANG WANG[1], XUANXUAN JI[2, 3], ZIYANG CHEN[1, 2], JIXIONG PU[1, 2*]

[1]College of Information Science and Engineering, Huaqiao University, Xiamen, Fujian 361021, People's Republic of China

[2]Fujian Provincial Key Laboratory of Light Propagation and Transformation, Huaqiao University, Xiamen, Fujian 361021, People's Republic of China

[3]College of Engineering, Niigata University, Niigata 950-2181, Japan

[*]Corresponding author: jixiong@hqu.edu.cn

We develop a *Q*-switched degenerate laser, delivering a partially coherent light pulse of duration about 16 ns. The spatial coherence of the output laser pulse can be varied by tuning the spatial filter inside the laser resonator, and the oscillating transverse mode structure can be determined by measuring the degree of coherence of the output laser pulse. It is shown that the larger is the diameter of the spatial filter, the more are the oscillating transverse modes, and the lower is the degree of coherence. Based on *coherent-mode representation* for the partially coherent source, we can estimate the transverse mode contribution to the output partially coherent laser. The experimental results on suppressing speckle demonstrate that the generated partially coherent light possesses the characteristics of rapid reduction of spatial coherence, making it an ideal source for high -speed imaging and ranging applications.

Keywords: partially coherent, degenerate laser, speckle suppress.

## 1. Introduction

Laser beams possess some special characteristics, such as high brightness, high direction and high coherence, enabling their applications in different areas. However, the laser beams with high coherence may produce harmful effects, such as speckle noise, resulting in low imaging quality [1–4]. The speckle noise seems detrimental to imaging applications and laser displays. It has been shown that an effective approach for suppressing the speckle noise is to reduce the coherence of illuminating laser beams. Several methods for reducing the coherence have been developed, such as passing the completely coherent laser beam through a rotating ground glass [5, 6], or through a spatial light modulator (SLM) or digital micromirror devices (DMD) [7–11]. The reduction of coherence is realized by taking the average of all independent states within a limited time interval. All these approaches seem defective, for instance, as the laser beam passes through the rotating ground glass, the speed of the rotating is very limited. This indicates that the speed of reducing coherence and suppression of speckle noise are not enough fast for some application areas. For instance, time-resolved optical imaging to observe fast dynamics, to achieve a rapid reduction of coherence is crucial for imaging applications. In other respect, the efficiency for obtaining partially coherent light by passing laser through a diffuser is quite low. Recently, several researchers have studied the lasers with a degenerate cavity, capable of generating laser beams with controllable spatial coherence by varying the diameter of a limiting spatial filter inside the resonator [12–17]. NIXON *et al*. proposed an efficient method to tune the spatial coherence of a degenerate laser [15]. KNITTER and his colleagues demonstrated a degenerate laser system that can be switched between a large number of mutually incoherent spatial modes and few-mode operation [4]. They performed dynamic multimodality biomedical imaging in *Xenopus* embryo hearts. It is shown that the multi-transverse-mode laser beams delivered from a degenerate cavity have the characteristics of the rapid reduction of spatial coherence. However, most degenerate lasers are operating in a continuous wave, or free-running modes. To achieve high power and/or fast temporal resolution, short pulse partially coherent laser light is crucial and necessary.

In this paper, we report, to the best of our knowledge, the first realization of $Q$-switched degenerate laser delivering ns pulse of partially coherent light with controllable spatial coherence. A spatially partially coherent laser beam of pulse width about 16 ns and single pulse energy 0.2 mJ is obtained. The oscillating transverse modes are changeable by tuning the spatial filter in the laser resonator, thereby regulating the spatial coherence of the output laser and the speckle contrast. The *coherent-mode representation* is used to obtain the mode structure of the output laser [18]. It will be shown that partially coherent light generated by this kind of laser possesses the characteristics of the rapid reduction of spatial coherence.

## 2. Experimental setup

The experimental setup is schematically shown in Fig. 1, in which a commercial diode -pumped Nd:YAG module (with length 120 mm and diameter 7 mm) is placed inside the laser resonator, acting as laser active medium. In the experiment, the pumping power is 76.2 W. Two flat plane mirrors M1 and M2 form a laser cavity, in which M1 and M2 are high reflective of 99.5% at 1064 nm. Two lenses of focal length $f = 200$ mm are placed inside the resonator to form a $4f$ telescope configuration, and in this case the laser resonator is called as degenerate one. The $4f$ arrangement ensures that any initial field distribution will be imaged onto itself after a single round trip, and therefore any field distribution is an eigenmode of the cavity. A size-variable spatial filter, which controls the number of oscillating modes, is inserted near the focus of L1 and L2. The $Q$-switched component is composed of a zero-order quarter-wave plate, a polarizing beam splitter cube and Pockels cell electro-optical switch made of KD*P which

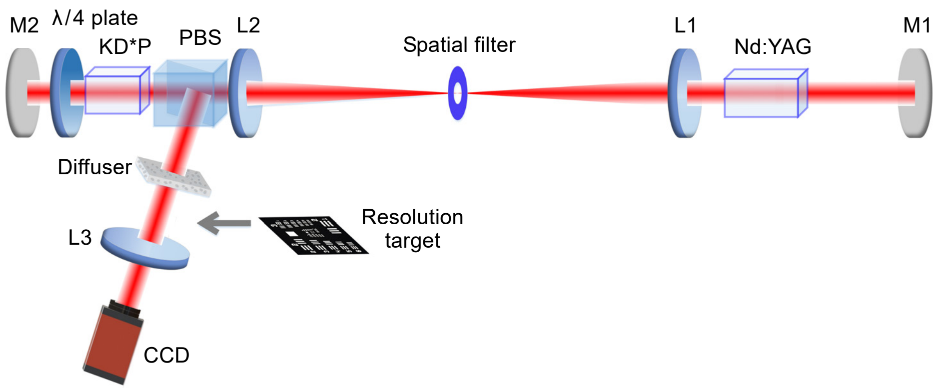


Fig. 1. The experimental setup of the *Q*-switched Nd:YAG laser. The degenerate laser consists of a gain medium Nd:YAG, two flat mirrors (M1 and M2), two lenses (L1 and L2), a quarter-wave plate, a polarizing beam splitter cube and Pockels cell electro-optical switch made of KD*P. The focal length of L1 and L2 is 200 mm. The number of lasing modes is controlled utilizing a variable spatial filter positioned at the focal plane between the two lenses. The output beam was detected by a CCD camera. To test the influence of the spatial coherence on reduction of speckles, a diffuser is placed in the test arm, and a resolution target is used to prove the benefit of low coherence in imaging.

is driven by electric pulses with a quarter-wave voltage of 3638 V and pulse width of 873 ns.

## 3. Experimental results

Degenerate cavity laser can support many transverse modes, therefore it is a good candidate for generating spatially partially coherent laser. Controlling the diameter (or radius) of the spatial filter will result in the changing of the oscillating transverse modes of the laser beam, leading to the change of the transverse mode of the output laser beam. It is well known that the beam radius of the high-order transverse modes along $x$-axis and $y$-axis are [19]

$$\omega_m(z) = \omega_0(z)\sqrt{2m+1} \tag{1}$$

$$\omega_n(z) = \omega_0(z)\sqrt{2n+1} \tag{2}$$

where $\omega_m(z)$, $\omega_n(z)$ and $\omega_0(z)$ are the radius of the high-order mode along $x$-axis, the high-order mode along $y$-axis, and the fundamental transverse mode, respectively. As shown in Eqs. (1) and (2), the higher order transverse mode has larger beam radius. This indicates that when the diameter (or radius) of the spatial filter is set to be small, the higher transverse mode has larger loss, so that higher transverse mode cannot oscillate. However when the diameter of the spatial filter is large, the loss of the higher order transverse mode gets small, so that the higher order transverse mode can oscillate. In this case, the laser can deliver many transverse modes.

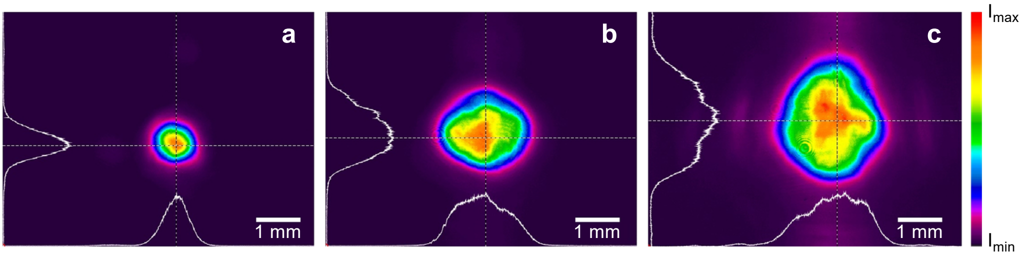


Fig. 2. The output laser beam patterns. Output beam patterns for the diameter of the limiting spatial filter are set to be (**a**) 1 mm, (**b**) 2 mm, and (**c**) 7.5 mm.

Figures 2**a**–2**c** present the laser beam patterns in the case that the diameter of the spatial filter is set to be 1, 2, and 7.5 mm, respectively. It is shown that with the increasing of the diameter of the spatial filter, the diameter of the output beam increases as well, due to more transverse modes existing in the degenerate cavity laser. The diameters of the output laser beams are measured to be 1.1, 1.7, and 2.2 mm, respectively.

In Fig. 3, we present the *Q*-switched pulses of the output laser, in the cases that the diameters of the spatial filter are 1, 2, and 7.5 mm, respectively. The pulse widths of

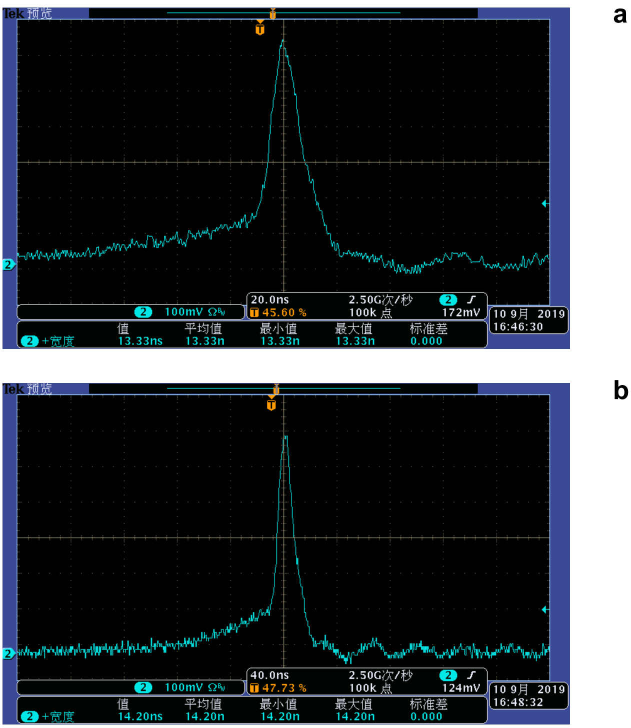


Fig. 3. The pulse shapes of the *Q*-switched laser. (**a**) The diameter of the limiting spatial filter $d = 1$ mm, the pulse width is 13.3 ns, (**b**) $d = 2$ mm, and the pulse width is 14.2 ns, (**c**) $d = 7.5$ mm, and the pulse width is 16.4 ns.

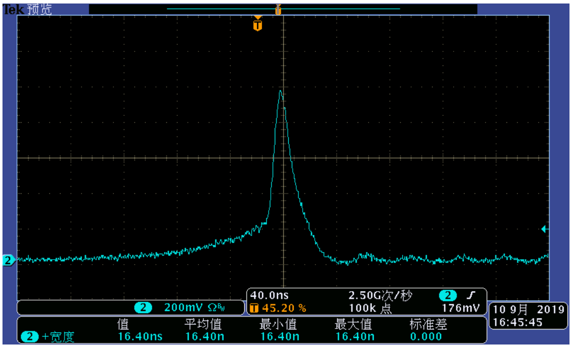


c

Fig. 3. Continued.

the output laser pulses are measured to be 13.3, 14.2, and 16.4 ns, respectively. This shows that the larger *Q*-switched pulse is obtained as the larger diameter of spatial filter within the laser cavity. Just as given in [20], when the loss of the *Q*-switched laser is lower, the pulse width is larger. Therefore when the diameter of the spatial filter is set to be largest, the loss of the laser is lowest, so that the pulse width is longest.

Now we investigate the ability to adjust the spatial coherence of the degenerate resonator laser by modulating the diameter of the spatial filter, and monitoring the ability to suppress speckles. The presence of a large number of transverse modes in the laser

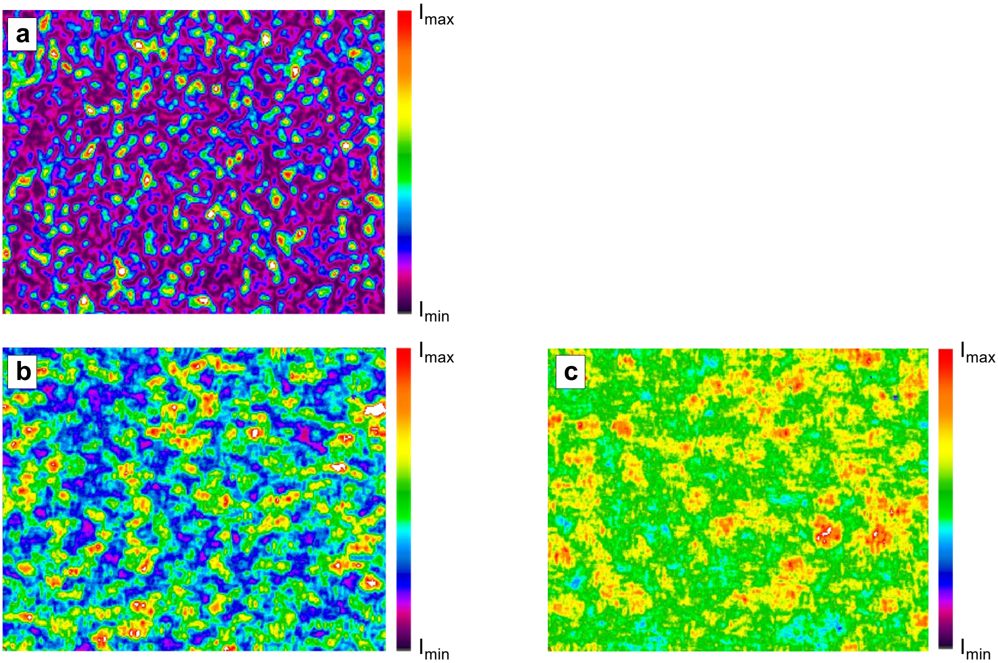


Fig. 4. The speckle patterns of the output laser light are detected by a CCD camera. (**a**) $d = 1$ mm, $C = 0.929$, (**b**) $d = 2$ mm, $C = 0.574$, and (**c**) $d = 7.5$ mm, $C = 0.184$.

emission reduces the spatial coherence. To confirm the speckle suppression, we placed a ground-glass diffuser into the laser beam and record the speckle patterns of transmitted light by a CCD camera, as shown in Fig. 1. The speckle patterns that are recorded by a CCD camera are illustrated in Fig. 4. The speckle patterns are recorded in one laser pulse, this is, the averaging over speckle is done in the duration of one laser pulse. To compare speckle patterns clearly, we calculate their speckle contrast $C$ as $C = \sigma/\langle I\rangle$, where $\sigma$ is the standard deviation and $\langle I\rangle$ is the mean of all pixel intensities in the image [21]. It is shown that when $d = 1$ mm, few transverse modes can oscillate, and the spatial coherence of the output laser is high, and the speckle contrast $C$ is quite large, reaching 0.929. When $d = 2$ mm, more transverse modes can oscillate in the laser cavity, and output laser has more transverse mode, resulting in a lower spatial coherence. In this case, $C = 0.574$. Moreover, when $d$ is largest, being 7.5 mm, much more transverse modes oscillate, and the speckle contrast $C$ is reduced to be 0.184. This means that the larger is the diameter of the spatial filter, the more transverse modes oscillate, and the smaller is the speckle contrast. As shown in Fig. 4**c**, suppression of the speckle is obtained within the duration of one $Q$-switched laser pulse (about 16 ns). *This indicates that the partially coherent laser light has the of rapid reduction of spatial coherence* [13].

The degenerate laser may provide a good source for generating partially coherent light with controllable spatial coherence, in which the spatial coherence can be changed by tuning the diameter of the spatial filter. Partially coherent light of low spatial coherence is shown to be advantageous, when used for high-intensity illumination source to realize the full-field imaging. To demonstrate this, we performed the experiments in which a resolution chart is placed after the random diffuser, and recorded by a CCD camera, as shown in Fig. 1. In Fig. 5, we give the image of the resolution chart, illuminated by the laser of highly spatial coherence (Fig. 5**a**), or that of low spatial coherence (Fig. 5**b**). We find that when the diameter of the limiting spatial filter is small ($d = 1$ mm), the spatial coherence of the output laser is quite high, and the imaging quality is poor.

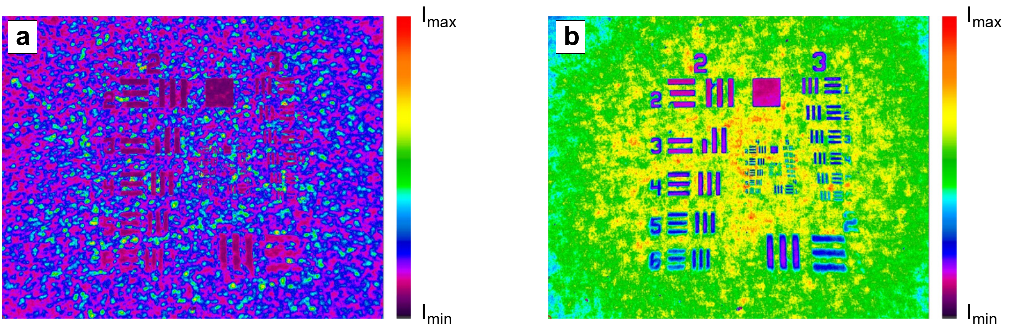


Fig. 5. Experimental demonstration of low-speckle imaging by using laser beams with different coherence. (**a**) The diameter of the limiting spatial filter is $d = 1$ mm, and the spatial coherence of the output laser beam is high. (**b**) The diameter of the limiting spatial filter is $d = 7.5$ mm, and the spatial coherence of the output laser beam is low. The speckle is largely reduced.

However, when $d = 7.5$ mm, the spatial coherence of the output laser is low, and the imaging quality is very good. It is noticed that the imaging is done within the duration of the one pulse, indicating that the spatial coherence of the output laser is of rapid reduction.

## 4. Coherent-mode representation for the output laser beams

In this paper, we focus our study on spatial coherence. We assume that the laser beam is of single frequency, for simplicity, and we neglect the frequency $\omega$ in following equations. The partially coherent laser can be characterized by a cross-spectral density of the form [22]

$$W(x_1, x_2) = [I(x_1)]^{1/2}[I(x_2)]^{1/2}\mu(x_1, x_2) \tag{3}$$

where $I(x)$ is the intensity, and $\mu(x_1, x_2)$ is the degree of coherence; $x_1$ and $x_2$ are two coordinate positions across the laser beam section. It is seen from Fig. 2 that the intensity distribution of the output laser beams is close to Gaussian distribution. This means that the intensity distribution can be approximately expressed as

$$I(x) = A\exp\left(-\frac{2x^2}{\sigma_I^2}\right) \tag{4}$$

where $A$ is a positive constant, representing the intensity at the center of the laser beam. $\sigma_I$ is the radius of the laser beam, in which the values of $\sigma_I$ can be evaluated from Fig. 2 to be 0.55, 0.85, and 1.1 mm, respectively, corresponding to the diameters of spatial filter $d = 1$, 2, and 7.5 mm, respectively. $\mu(x_1, x_2)$ is a degree of coherence, and is assumed to be of the form

$$\mu(x_1, x_2) = \mu(\Delta x) \tag{5}$$

here $\Delta x = x_1 - x_2$. Equation (5) indicates that the degree of coherence is dependent on $x_1$ and $x_2$, only through $\Delta x$. The degree of coherence of the output laser beam can be measured by the Young's two-pinhole interference experiment, as shown in Fig. 6. It is shown that the light coming from two pinholes Q1 and Q2 interferes at point $P$. It has been found that if the intensities at point $P$ coming from Q1 and Q2 are the same, the visibility of the interference fringes is just equal to the module of the degree of coherence, *i.e.*, [22]

$$v(P) = \frac{I_{\max} - I_{\min}}{I_{\max} + I_{\min}} = |\mu(x_1, x_2)| = |\mu(\Delta x)| \tag{6}$$

where $x_1$ and $x_2$ are the coordinates of the two different positions, Q1 and Q2. $I_{\max}$ and $I_{\min}$ are the maximum intensity and minimum intensity of the interference fringes.

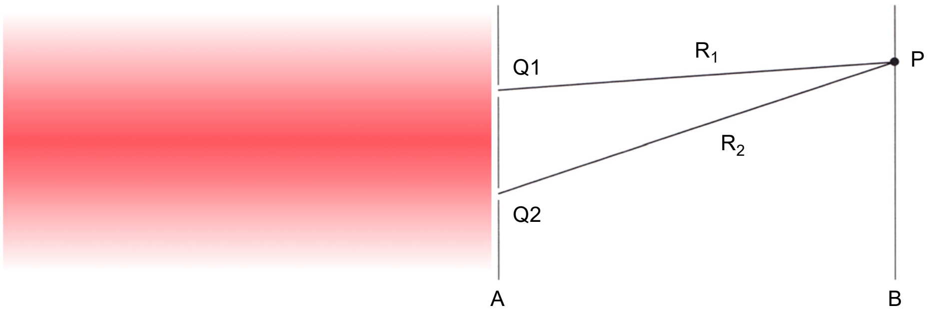


Fig. 6. Notation relating to Young's two-pinhole interference experiment for measuring the degree of coherence of the output laser beam.

Equation (3) indicates that the visibility of the interference fringes is just equal to the degree of coherence. Therefore, by measuring the visibility of the interference fringes, we can obtain the degree of coherence of the output laser beam.

To measure the degree of coherence, we choose different two-pinholes with distances of 0.2, 0.4, 0.6, and 0.8 mm, respectively. In Fig. 7, we present the degree of coherence as a function of the distances between two-pinholes, Q1 and Q2. For simplicity, the measurement is performed for the two pinholes moving along $x$-axis of the laser beam section. In Fig. 7, three curves correspond to the diameters of the limiting spatial filter are 1, 2, and 7.5 mm, respectively. It is found that the larger is the diameter, the lower is the spatial coherence. The insets are the interference fringes, in which the distance between two-pinholes is 0.4 mm, and the diameters of the spatial filter are 1, 2, and 7.5 mm, respectively. Clearly, the smaller is the diameter, the sharper are the interfer-

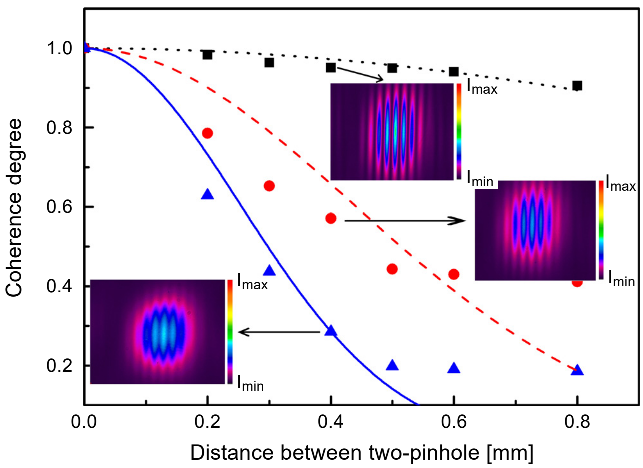


Fig. 7. The degree of coherence as a function of the distance of the two-pinholes for three different diameters of the spatial filter. The black squares with dotted line denote the result for a spatial filter diameter of 1 mm, the red circles with dashed line denote the result for a spatial filter diameter of 2 mm and the blue triangles with solid line denote the result for a spatial filter diameter of 7.5 mm.

ence fringes, and the larger is the spatial coherence. And the spatial coherence decreases with the increment of the distance between two pinholes. The spatial coherence varying with $\Delta x$ is called the degree of coherence. We find that, for a fixed diameter, the function of spatial coherence with $\Delta x = x_1 - x_2$ can approximately be described as a Gaussian one. Therefore, the fitting function of the three curves (degree of coherence) in Fig. 7 is given by

$$\mu(\Delta x) = \exp\left(-\frac{2\Delta x^2}{\sigma_\mu^2}\right) \tag{7}$$

where the fitting parameters are $\sigma_\mu = 3.37747$, 0.8732, and 0.5056 mm, respectively, corresponding to the diameters of spatial filter $d = 1$, 2, and 7.5 mm, respectively.

According to the theory of the *coherent-mode representation*, the cross-spectral density of the output partially coherent laser beams may be represented in the form [18]

$$W(x_1, x_2) = \sum_n \lambda_n \varphi_n^*(x_1)\varphi_n(x_2), \qquad n = 0, 1, 2, ... \tag{8}$$

where $\varphi_n$ are the eigenfunctions, and $\lambda_n$ are the eigenvalues of the Fredholm integral equation

$$\int_D W(x_1, x_2)\varphi_n(x_1)\mathrm{d}^3 x_1 = \lambda_n \varphi_n(x_2) \tag{9}$$

The eigenfunctions may be taken to be orthonormalized over the domain $D$, *i.e.*,

$$\int_D \varphi_n^*(x)\varphi_n(x)\mathrm{d}^3 r = \delta_{nm} \tag{10}$$

where $\delta_{nm}$ is the Kronecker symbol ($\delta_{nm} = 1$ when $n = m$, $\delta_{nm} = 0$ when $n \neq m$). $\varphi_n(x)$ can be viewed as the transverse modes of a laser, such as Hermite–Gaussian modes. The quantities $\lambda_n$ are positive, and are weighted factor of the transverse mode. It is found from Eq. (8) that the output partially coherent laser is composed of many transverse modes $\varphi_n(x)$. To describe the related contribution to the partially coherent laser, we define the ratio of the eigenvalues $\lambda_n$ to the lowest eigenvalues $\lambda_0$, *i.e.*, $\lambda_n/\lambda_0$.

Based on the above equations, we can calculate the distribution of the modes by the degree of coherence. The results are presented in Fig. 8. As shown in Fig. 8**a**, the diameter of the spatial filter is smallest ($d = 1$ mm), the degree of coherence is very high, only two transverse modes exist, *i.e.*, the fundamental transverse mode, and first -order transverse mode. It is seen that the fundamental transverse mode is very strong, compared to the first-order transverse mode. When the diameter of the spatial filter is chosen to be 2 mm, the degree of coherence becomes small, and more transverse modes can oscillate in the laser cavity. As shown in Fig. 8**b**, five transverse modes can oscillate, and the fundamental transverse mode is strongest, and the higher-order transverse

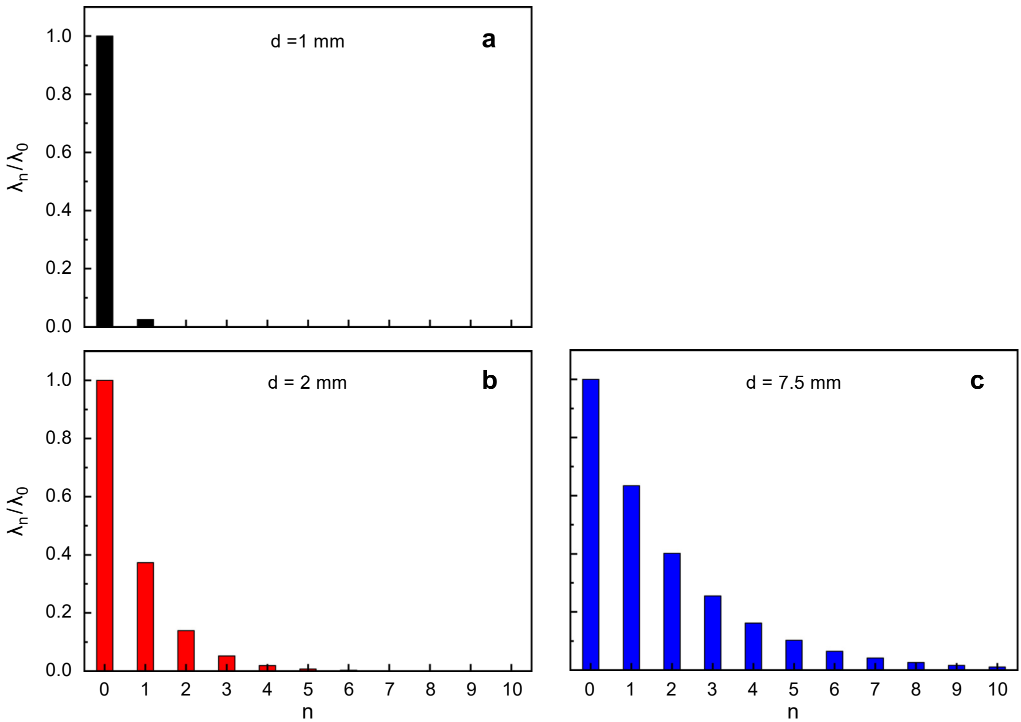


Fig. 8. Distribution of transverse modes. The diameter of spatial filter is set to: (**a**) $d = 1$ mm, (**b**) $d = 2$ mm, and (**c**) $d = 7.5$ mm.

mode gets weaker intensity. In Fig. 8**c**, we present the transverse mode distribution of the output laser, in which the diameter of the spatial filter is largest, being $d = 7.5$ mm. In this case, the degree of coherence is smallest, and the number of the oscillating transverse modes is most. The oscillating modes are eleven. As described above, we measured the degree of coherence only along $x$-axis. It is assumed that the laser beam is symmetric, the total number of the transverse modes should be the square of the transverse mode number along one direction. Therefore, when $d = 7.5$ mm, the total transverse mode number reaches 121.

## 5. Conclusion

We have constructed a $Q$-switched degenerate laser, delivering a partially coherent light pulse of duration about 16 ns. The spatial coherence could be changed by tuning the diameter of the spatial filter inside the laser cavity. The larger diameter of the spatial filter resulted in more transverse modes oscillating in the laser. The transverse mode distribution has been evaluated, more than 121 transverse modes existed when the diameter of the spatial filter is largest, being 7.5 mm. It has been found that the changing of the diameter of the spatial filter not only results in the oscillating transverse mode number, but also the pulse duration. The experimental results on suppressing the speckles demonstrate that the generated partially coherent light has the characteristics of rapid reduction of spatial coherence. This kind of partially coherent laser is an ideal source for high-speed imaging and ranging applications.

*Acknowledgements* – This research work is supported by the National Science Foundation of China (NSF) under the grant number 61575070 and 11674111.

## References

[1] REDDING B., CHOMA M.A., CAO H., *Speckle-free laser imaging using random laser illumination*, Nature Photonics **6**(6), 2012, pp. 355–359, DOI: 10.1038/nphoton.2012.90.

[2] CAO H., CHRIKI R., BITTNER S., FRIESEM A.A., DAVIDSON N., *Complex lasers with controllable coherence*, Nature Reviews Physics **1**(2), 2019, pp. 156–168, DOI: 10.1038/s42254-018-0010-6.

[3] AKRAM M.N., TONG Z.M., OUYANG G.M., CHEN X.Y., KARTASHOV V., *Laser speckle reduction due to spatial and angular diversity introduced by fast scanning micromirror*, Applied Optics **49**(17), 2010, pp. 3297–3304, DOI: 10.1364/AO.49.003297.

[4] KNITTER S., LIU C.G., REDDING B., KHOKHA M.K., CHOMA M.A., CAO H., *Coherence switching of a degenerate VECSEL for multimodality imaging*, Optica **3**(4), 2016, pp. 403–406, DOI: 10.1364/OPTICA.3.000403.

[5] WANG F., LIU X.L., YUAN Y.S., CAI Y.J., *Experimental generation of partially coherent beams with different complex degrees of coherence*, Optics Letters **38**(11), 2013, pp. 1814–1816, DOI: 10.1364/OL.38.001814.

[6] CHEN H., JI X., WANG Y., CHEN Z., SASAKI O., PU J., *Investigation on intracavity SHG with controllable coherence in a degenerate laser*, IEEE Journal of Quantum Electronics **56**(1), 2020, article 1700106, DOI: 10.1109/JQE.2019.2958372.

[7] CHANG C.C., CHEN X.D., CHEN Z.Y., LIN Z., LI X.Y., PU J.X., *Experimental investigation on a nonuniformly correlated partially coherent laser*, Applied Optics **57**(16), 2018, pp. 4381–4385, DOI: 10.1364/AO.57.004381.

[8] HUANG T.D., LU T.H., *Controlling an optical vortex array from a vortex phase plate, mode converter, and spatial light modulator*, Optics Letters **44**(16), 2019, pp. 3917–3920, DOI: 10.1364/OL.44.003917.

[9] CUI S.W., CHEN Z.Y., ZHANG L., PU J.X., *Experimental generation of nonuniformly correlated partially coherent light beams*, Optics Letters **38**(22), 2013, pp. 4821–4824, DOI: 10.1364/OL.38.004821.

[10] WANG Y.X., MENG P.H., WANG D.Y., RONG L., PANEZAI S., *Speckle noise suppression in digital holography by angular diversity with phase-only spatial light modulator*, Optics Express **21**(17), 2013, pp. 19568–19578, DOI: 10.1364/OE.21.019568.

[11] CHEN X.D., CHANG C.C., CHEN Z.Y., LIN Z.L., PU J.X., *Generation of stochastic electromagnetic beams with complete controllable coherence*, Optics Express **24**(19), 2016, pp. 21587–21596, DOI: 10.1364/OE.24.021587.

[12] ARNAUD J.A., *Degenerate optical cavities*, Applied Optics **8**(1), 1969, pp. 189–195, DOI: 10.1364/AO.8.000189.

[13] CHRIKI R., MAHLER S., TRADONSKY C., PAL V., FRIESEM A.A., DAVIDSON N., *Spatiotemporal supermodes: rapid reduction of spatial coherence in highly multimode lasers*, Physical Review A **98**(2), 2018, article 023812, DOI: 10.1103/PhysRevA.98.023812.

[14] LIEW S.F., KNITTER S., WEILER S., MONJARDIN-LOPEZ J.F., RAMME M., REDDING B., CHOMA M.A., CAO H., *Intracavity frequency-doubled degenerate laser*, Optics Letters **42**(3), 2017, pp. 411–414, DOI: 10.1364/OL.42.000411.

[15] NIXON M., REDDING B., FRIESEM A.A., CAO H., DAVIDSON N., *Efficient method for controlling the spatial coherence of a laser*, Optics Letters **38**(19), 2013, pp. 3858–3861, DOI: 10.1364/OL.38.003858.

[16] CHRIKI R., NIXON M., PAL V., TRADONSKY C., BARACH G., FRIESEM A.A., DAVIDSON N., *Manipulating the spatial coherence of a laser source*, Optics Express **23**(10), 2015, pp. 12989–12997, DOI: 10.1364/OE.23.012989.
[17] NIXON M., KATZ O., SMALL E., BROMBERG Y., FRIESEM A.A., SILBERBERG Y., DAVIDSON N., *Real-time wavefront shaping through scattering media by all-optical feedback*, Nature Photonics **7**(11), 2013, pp. 919–924, DOI: 10.1038/nphoton.2013.248.
[18] STARIKOV A., WOLF E., *Coherent-mode representation of Gaussian Schell-model sources and of their radiation fields*, Journal of the Optical Society of America **72**(7), 1982, pp. 923–928, DOI: 10.1364/JOSA.72.000923.
[19] LUXON J.T., PARKER D.E., *Practical spot size definition for single higher-order rectangular-mode laser beams*, Applied Optics **20**(10), 1981, pp. 1728–1729, DOI: 10.1364/AO.20.001728.
[20] DEGNAN J.J., *Optimization of passively Q-switched lasers*, IEEE Journal of Quantum Electronics **31**(11), 1995, pp. 1890–1901, DOI: 10.1109/3.469267.
[21] REDDING B., AHMADI P., MOKAN V., SEIFERT M., CHOMA M.A., CAO H., *Low-spatial-coherence high-radiance broadband fiber source for speckle free imaging*, Optics Letters **40**(20), 2015, pp. 4607–4610, DOI: 10.1364/OL.40.004607.
[22] WOLF E., *Introduction to the Theory of Coherence and Polarization of Light*, Cambridge University Press, 2007, Chapter 3.

*Received April 27, 2020*
*in revised form June 9, 2020*